72. 1-(2′-Deoxy-β-D-xylofuranosyl)thymine Building Blocks for Solid-Phase Synthesis and Properties of Oligo(2′-Deoxyxylonucleotides)

by **Helmut Rosemeyer** and **Frank Seela***

Laboratorium für Organische und Bioorganische Chemie, Fachbereich Biologie/Chemie, Universität Osnabrück, Barbarastr. 7, D-4500 Osnabrück

(22.III.91)

1-(2′-Deoxy-β-D-*threo*-pentofuranosyl)thymine (= 1-(2′-deoxy-β-D-xylofuranosyl)thymine; xT_d; **2**) was converted into its phosphonate **3b** as well as its 2-cyanoethyl phosphoramidite **3c**. Both compounds were used for solid-phase synthesis of d[$(xT)_{12}$-T] (**5**), representing the first DNA fragment build up from 3′–5′-linked 2′-deoxy-β-D-xylonucleosides. Moreover, xT_d was introduced into the innermost part of the self-complementary dodecamer d(G-T-A-G-A-A-xT-xT-C-T-A-C)$_2$ (**9**). The CD spectrum of d[$(xT)_{12}$–T] (**5**) exhibits reversed *Cotton* effects compared to d(T_{12}) (**6**; see *Fig. 1*), implying a left-handed single strand. With d(A_{12}) (**7**) it could be hybridized to form a propably left-handed double strand d(A_{12})·d[$(xT)_{12}$–T] (**7**·**5**) which was confirmed by melting experiments in combination with temperature-dependent CD spectroscopy. While **5** was hydrolyzed by snake-venom phosphodiesterase, it was resistant towards calf-spleen phosphodiesterase. The modified, self-complementary duplex **9** was hydrolyzed completely by snake-venom phosphodiesterase, at a twelvefold slower rate compared to unmodified **8**; calf-spleen phosphodiesterase hydrolyzed **9** only partially.

Introduction. – Synthetic oligonucleotides build up from nucleotide units with a configurationally altered D-ribofuranose or a D-ribopyranose moiety are of interest with respect to unusual DNA structures as well as to their stability towards cellular nucleases. *i*) [α-D]-DNA – consisting exclusively of α-D-configurated purine and pyrimidine 2′-deoxyribonucleosides – remain intact upon the action of nuclease S1 and calf-spleen phosphodiesterase [1]. *ii*) Oligonucleotides containing β-D-ribopyranosyl-nucleotide units have extraordinary structural and chemical properties [2]. *iii*) Hitherto unknown, however, are oligonucleotides in which the OH group at C(3′) of the naturally occurring 2′-deoxy-β-D-ribofuranosyl-nucleotide units shows 3′,4′-*threo*-configuration. Only two isomeric dinucleoside monophosphates containing 1-(2′-deoxy-β-D-*threo*-pentofuranosyl)thymine (= 1-(2′-deoxy-β-D-xylofuranosyl)thymine; xT_d; **2**) have been synthesized recently [3].

Here, we report for the first time on oligonucleotides containing 1-(2′-deoxy-β-D-xylofuranosyl)thymine (**2**). For this purpose, building blocks for automated solid-phase synthesis were prepared which allow the incorporation of this nucleoside into any position of an oligonucleotide chain. Furthermore, the oligo(2′-deoxyxylonucleotides) were studied with respect to their structure and base-pairing with complementary oligo(dA).

Results and Discussion. – *Syntheses of Building Blocks of* **2** *and Incorporation into Oligonucleotides.* The synthesis of 1-(2′-deoxy-β-D-*threo*-pentofuranosyl)thymine (xT_d; **2**) was performed according to *Fox* and *Miller* [4] starting from 2′-deoxythymidine (**1**). Protection of **2** with 4,4′-dimethoxytriphenylmethyl chloride ($(MeO)_2TrCl$) in the pres-

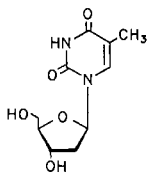

1

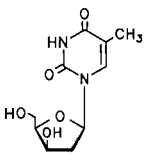

2

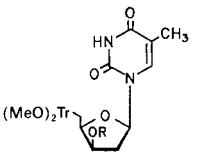

3a R = H
b R = –PH(O)O⁻Et₃NH⁺
c R = –P[(i-Pr)₂N](OCH₂CH₂CN)

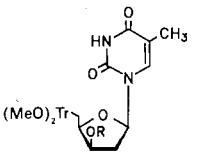

4a R = C(O)CH₂CH₂COOH
b R = C(O)CH₂CH₂COO(4-nitrophenyl)
c R = C(O)CH₂CH₂CONH···CPG

d[(xT)₁₂-T]
5

d(T₁₂)
6

d(A₁₂)
7

d(G-T-A-G-A-A-T-T-C-T-A-C)₂
8

d(G-T-A-G-A-A-xT-xT-C-T-A-C)₂
9

ence of *Hünig*'s base afforded the 5′-$(MeO)_2$Tr derivative **3a**. Subsequent treatment with PCl_3/*N*-methylmorpholine/1,2,4-triazole gave the phosphonate **3b** which was isolated as triethylammonium salt [5]. New compounds were characterized by ^{1}H- and ^{13}C-NMR spectra as well as elemental analyses.

As *Table 1* shows, the ^{13}C-NMR spectra of 3′-epimeric compounds exhibit significant upfield shifts of C(3′), C(4′), and C(5′) (1–2.5 ppm) and a downfield shift of C(2′) on changing the configuration from 3′,4′-*erythro* to 3′,4′-*threo* (**1** → **2**). As ^{13}C-NMR signals are sensitive to variations of torsion angles, the sugar puckering of both, 2′-deoxythymidine (**1**) and 1-(2′-deoxy-β-D-xylofuranosyl)thymine (**2**), was determined. Applying the pseudorotational analysis [6] [7] of vicinal H,H couplings of the corresponding glyconic moieties and using the pseudorotational parameters of 2′-deoxy-β-D-ribofuranosyl- as well as of -xylofuranosyl moieties [8], the ^3J(H–C(1′), H_β–C(2′)) coupling constants can be used to assess the *N*- and *S*-conformer populations of both nucleosides.

Table 1. *^{13}C-NMR Chemical Shifts of Nucleosides*[a])

	C(2)	C(4)	C(5)	C(6)	C(1′)	C(2′)	C(3′)	C(4′)	C(5′)	Me
1	150.6	136.2	109.4	163.8	83.8	39.5	70.5	87.3	61.5	12.4
2	150.6	137.3	108.7	163.9	83.5	40.8	68.7	84.9	59.6	12.6
$[(MeO)_2Tr]T_d$	150.5	135.8	109.7	163.8	83.8	39.9	70.6	86.5	64.1	11.9
3a	150.6	136.9	108.4	163.9	83.5	40.9	69.1	84.3	62.9	12.5
$T_{d\psi}$[b])	150.5	135.6	109.8	163.7	83.9	40.6	72.7	84.5	63.6	11.7
3b	150.7	136.9	108.8	163.9	83.7	40.6	71.4	82.5	62.5	11.5

[a]) Measured in (D_6)DMSO at 296 K; resonances of protecting groups are not given.
[b]) ψ = 3′-phosphonate.

2′-Deoxythymidine (^3J(H–C(1′), H_β–C(2′)) = 6.7 Hz) shows a 58% *S*-type sugar puckering, while the corresponding 3′,4′-*threo*-configurated diastereoisomer **2** (^3J(H–C(1′), H_β–C(2′)) = 2.7 Hz) reveals 84% *N*-type sugar conformation. This change in the preferred sugar conformation was confirmed by 1D ^{1}H-NOE difference spectroscopy on **2**: Irradiation of H–C(1′) does only result in NOE's at H–C(4′) (3.0%) and H_α–C(2′) (6.7%), but not at H–C(3′), although both protons are positioned on the α-face of the glyconic moiety. This has to be interpreted by a pronounced population of the twist conformer $^3T_{2'}$ (*N*-type) [9]. Epimerization of the 3′-OH group of **1** in combination with a change of the preferred sugar conformation brings this group in **2** into close contact to the nucleobase as well as the 5′-CH_2OH group as the 'axial-down' orientation is changed into 'axial-up'. This may also explain the ^{31}P-NMR resonance of 3′,4′-*threo*-configurated **3b** which is shifted to higher field compared to regular 3′,4′-*erythro*-configurated phosphonates ($\Delta\delta$ = 0.2–0.3 ppm).

Alternatively to phosphonate **3b**, the 2-cyanoethyl phosphoramidite **3c** was synthesized from **3a** by reaction with chloro(2-cyanoethoxy)(diisopropylamino)phosphane [10]. Interestingly, both diastereoisomers revealed sufficiently different chromatographic mobilities and could be partially separated. The faster migrating compound was then correlated with the upfield ^{31}P-NMR signal (148.5 ppm) and the slower migrating one with the downfield resonance (151.8 ppm). Moreover, the ^{31}P-resonances of the diastereoisomers of **3c** differ by 3.2 ppm which is significantly larger then in the case of a 3′,4′-*erythro*-configurated phosphoramidite ($\Delta\delta$ = 0.2–0.5 ppm). Again, different shieldings may be explained by different steric interactions between the nucleobase and/or the 5′-CH_2OH group and the enantiomeric phosphoramidite moiety.

Succinylation of **3a** in the presence of 4-(dimethylamino)pyridine gave acid **4a** which was subsequently activated by formation of its 4-nitrophenyl ester **4b** and then coupled to amino-functionalized, controlled pore glass (→**4c**) [11]. The ligand concentration in **4c** was determined to be 50.4 μmol of **2**/g of *Fractosil*.

The phosphonate **3b** was then employed in automated DNA synthesis on solid support of the oligonucleotides **5** and **9**. For the synthesis of **5**, silica-gel-bound 2′-deoxythymidine was used yielding an oligonucleotide with a 3′-pending 3′,4′-*erythro*-configurated 2′-deoxythymidine but with twelve identical internucleotide linkages. The protocol of detritylation, activation (adamantanoyl chloride), coupling, and capping followed a protocol described recently [5]. Oxidation with I_2 in pyridine/H_2O/THF was carried out on the oligomeric level. Alternatively, 2-cyanoethyl phosphoramidite **3c** was used for preparation of **5** [10]. The oligonucleotides were removed from the support according to [10]. The 5′-protected oligonucleotides were then purified by reversed-phase HPLC, and the detritylated compounds (80% AcOH/H_2O) again submitted to reversed-phase HPLC and lyophilized.

Properties of Oligo(deoxyxylonucleotides). *Fig. 1* shows the CD spectra of $d(T_{12})$ (**6**) and $d[(xT)_{12}-T]$ (**5**) in 1M NaCl. While **6** exhibits a B_{2u} transition at 274 nm with positive

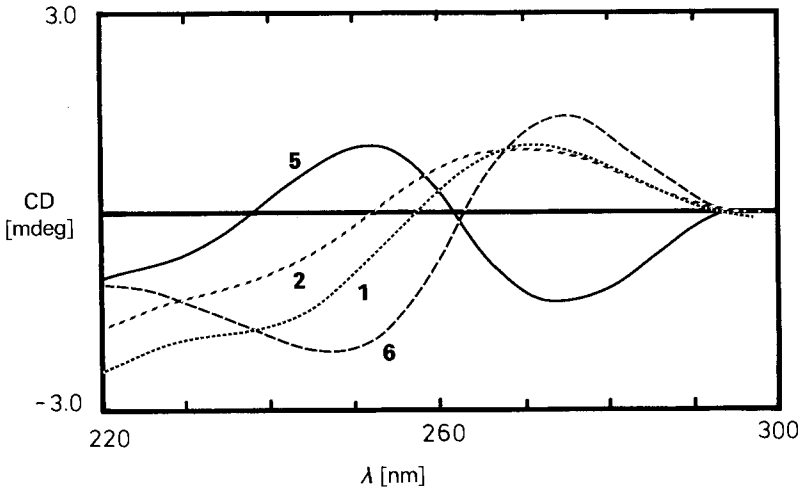

Fig. 1. *CD Spectra of* $d(T_{12})$ (**6**; ----), T_d (**1**; ·····), xT_d (**2**; -----), *and* $d[(xT)_{12}-T]$ (**5**; ——). Oligomer conc., 2.2 μM; monomer conc., 27 μM; measured in 60 mM cacodylate buffer (pH 7.0), 1M NaCl, 100 mM $MgCl_2$, at 8°.

and a B_{1u} transition at 247 nm with negative sign, the corresponding π–π^* transitions of the modified oligonucleotide **5** show reversed *Cotton* effects together with a bathochromic shift (6 nm) of the B_{1u} band. The 1-(2′-deoxy-β-D-*threo*-pentofuranosyl)thymine (**2**) as well as the parent nucleoside **1**, however, display only a positive *Cotton* effect at 267 nm.

It is known from X-ray analysis of d(pT–T) as well as NMR spectroscopy that poly(T_d) adopts a single-stranded, right-handed helix in which the bases are turned out and, therefore, not stacked [12]. Due to these reasons, it is likely that d[$(xT)_{12}$–T] (**5**) adopts a left-handed helical single strand similar to the strands of a Z-DNA. Stable Z-DNA under low salt concentration conditions can only be produced by chemical modifications. If, *e.g.*, guanine residues of poly(dG–dC) are substituted in position 8 by Br, '*syn*'-orientation of the purine base and hence the Z-DNA form is preferred, even at low salt concentrations [13]. In **5**, the change of the C(3′)-configuration of the monomeric unit seems to induce a stable left-handed single strand, even under nearly physiological conditions. This particular secondary structure proves stable, even if the salt concentration is raised to 4M NaCl.

Next, we proved that d[$(xT)_{12}$–T] (**5**) is able to form a stable 1:1 complex with d(A_{12}) (**7**) and compared its melting and CD-spectroscopic characteristics with those of d(A_{12})·d(T_{12}) (**7**·**6**). As *Fig. 2a* demonstrates, a mixture of **7** and **5** in a molar ratio of 1:1 shows a strongly cooperative melting profile (260 nm) with a T_m of 36 ± 1° and a thermal hypochromicity between 10 and 80° of 18% (see *Table 2*). In comparison to this, **7**·**6** exhibits a melting point of 43 ± 1° and a thermal hypochromicity of 32% (*Table 2*). Neither **7**, **6**, nor **5** show cooperative melting under identical experimental conditions (see *Table 2*). These results clearly demonstrate hybrid formation between the regular d(A_{12}) strand and its modified counterpart d[$(xT)_{12}$ – T], *i.e.* **7**·**5**, but with a different

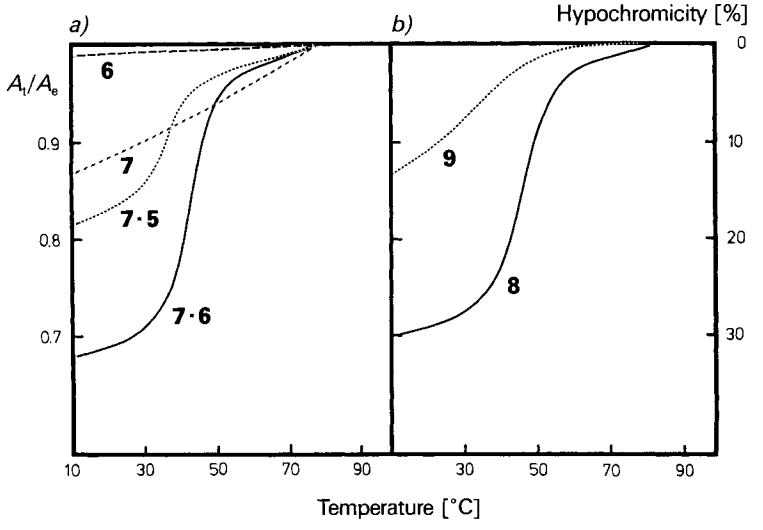

Fig. 2. *Normalized melting profiles* a) *of d(A_{12})·d(T_{12})* (**7**·**6**), *d(A_{12})·d[$(xT)_{12}$-T]* (**7**·**5**), *d(A_{12})* (**7**), *and d(T_{12})* (**6**; oligomer conc., 2 μM of single strands) *and* b) *of d(G-T-A-G-A-A-T-T-C-T-A-C)$_2$* (**8**) *and d(G-T-A-G-A-A-xT-xT-C-T-A-C)$_2$* (**9**; oligomer conc., 1.2 μM of double strands). Buffer, see *Fig. 1*.

Table 2. T_m *Values and Hypochromicities of Oligonucleotides*

Oligonucleotide	Thermal hypochromicity[a]) [%] (10–80°, 260 nm)	Enzymatic hypochromicity[b]) (snake-venom phosphodiesterase)	T_m[a]) [°C]
$d(A_{12})$ (**7**)	13	30	[c])
$d(T_{12})$ (**6**)	1–2	4	[c])
$d[(xT)_{12} - T]$ (**5**)	1–2	4	[c])
$d(A_{12}) \cdot d(T_{12})$ (**7·6**)	32	–	43
$d(A_{12}) \cdot d[(xT)_{12} - T]$ (**7·5**)	18	–	36
d(G-T-A-G-A-A-T-T-C-T-A-C)$_2$ (**8**)	30	35	46
d(G-T-A-G-A-A-xT-xT-C-T-A-C)$_2$ (**9**)	14	16	35

[a]) Measured in 60 mM cacodylate buffer, pH 7.0, 1M NaCl, 100 mM $MgCl_2$.
[b]) Measured in 0.1M *Tris*-HCl buffer, pH 8.3.
[c]) No cooperative melting.

secondary structure as compared to the parent duplex $d(A_{12}) \cdot d(T_{12})$ (**7·6**). Triple-strand formation – as has been demonstrated for oligo(dA)·oligo(dT) at 2M NaCl and/or 50 mM $MgCl_2$ – was ruled out for our measuring conditions by additional melting experiments at 284 nm which was reported to be an isosbestic point of the UV spectra of native and melted $d(A_{12}) \cdot d(T_{12})$ duplex [14]. Also under our measuring conditions, no change in UV absorbance at 284 nm was observed for the duplexes **7·5** and **7·6** (data not shown).

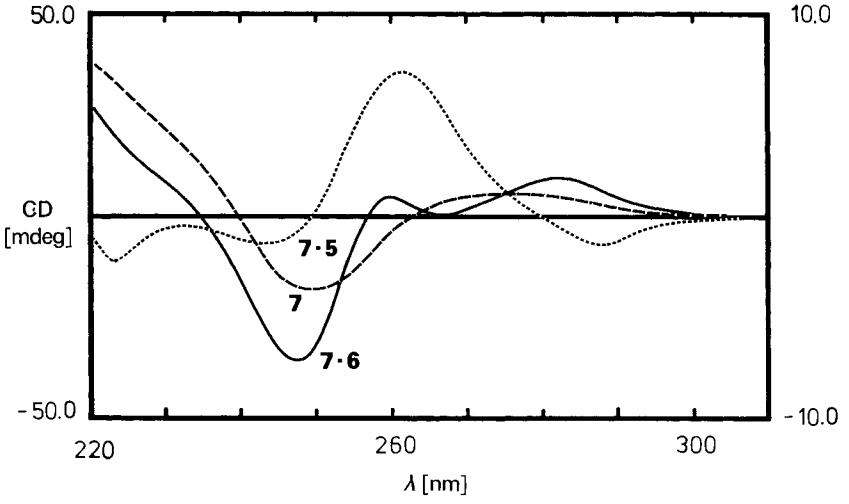

Fig. 3. *CD Spectra of* $d(A_{12}) \cdot d(T_{12})$ (**7·6**; —— left ordinate), $d(A_{12})$ (**7**; ----, right ordinate), *and* $d(A_{12}) \cdot d[(xT)_{12} - T]$ (**7·5**; -----, right ordinate). Equimolar amounts of single strands (2 μM, each) were hybridized; conc. of $d(A_{12})$ (**7**) 3.3 μM; temp., 8°; buffer, see *Fig. 1*.

Complex formation between **5** and **7** was confirmed by CD spectroscopy. *Fig. 3* presents the CD spectra of $d(A_{12})$ (**7**), $d(A_{12}) \cdot d(T_{12})$ (**7·6**) as well as of $d(A_{12}) \cdot d[(xT)_{12} - T]$ (**7·5**) in cacodylate buffer (60 mM, pH 7.0, 1M NaCl, 100 mM $MgCl_2$). As can be seen, **7·5** exhibits a characteristic spectrum being completely different from those of the parent duplex **7·6** as well as of the corresponding single strands. The ellipticity of the positive

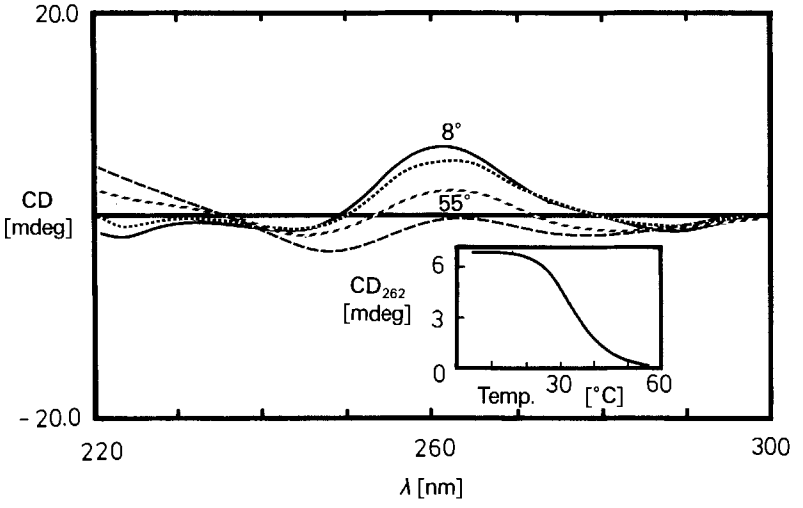

Fig. 4. *CD Spectra of* $d(A_{12})\cdot d[(xT)_{12}-T]$ (**7·5**; 2 μM single-strand conc.) *at temperatures between 8 and 55°.* Buffer, see *Fig. 1.* Insert: ellipticity at 262 nm as a function of temp.

Cotton effect at 262 nm is strongly temperature-dependent reflecting the melting process of the duplex, while the negative *Cotton* band at 288 nm is hypsochromically shifted (10–12 nm) when going from 8 to 55° (*Fig. 4*). The general pattern of the CD spectrum of **7·5** corresponds to that of a Z-like DNA [15]. This implies that the hybrid formation between the right-handed $d(A_{12})$ single-stranded helix with a left-handed $d[(xT)_{12}-T]$ single-stranded helix results in a left-handed double helix.

In the following, we synthesized the self-complementary dodecamer d(G-T-A-G-A-A-T-T-C-T-A-C)$_2$ (**8**) and substituted the innermost T_d's by xT_d. The resulting oligonucleotide **9** still forms a hybrid with a T_m of 35 ± 1° and a thermal hypochromicity (10–80°) of 14% (*Table 2*). Compared to the parent duplex **8** (T_m, 46 ± 1°; melting hypochromicity, 30%), the melting curve of **9** (*Fig. 2b*), however, shows only a slight cooperativity implying an inhomogeneous secondary structure. The CD spectra of both, **8** and **9**, however, show a very similar pattern [16], but the ellipticity values of the modified **9** are slightly reduced (*Fig. 5*). Moreover, a slight hypsochromic shift (*ca.* 3 nm) of the B_{2u} transition of **9** is observed compared to **8**. Increasing the temperature to 55° (20° above T_m of **9**) does not alter the pattern of the CD spectrum of **9** significantly (*Fig. 5*). These results can be interpreted by formation of a B-DNA-like structure for **9** in which two double-helical tetramers are interrupted by a central tetramer (d(A-A-xT-xT)$_2$) which might be either looped out or forms a duplex with a different secondary structure. According to the CD spectra of the oligomers, parallel or antiparallel arrangement of the oligonucleotides within the structure is possible. Further experiments are necessary to assign their structure in detail.

In the following, we tested the enzymatic hydrolysis of $d[(xT)_{12}-T]$ (**5**) by snake-venom phosphodiesterase (oligonucleotide-5′-nucleotidohydrolase) followed by alkaline phosphatase as well as by calf-spleen phosphodiesterase (oligonucleotide-3′-nucleotidohydrolase) and alkaline phosphatase. HPLC analysis shows that **5** was cleaved by snake-venom phosphodiesterase completely (*Fig. 6b*), while it was resistant towards

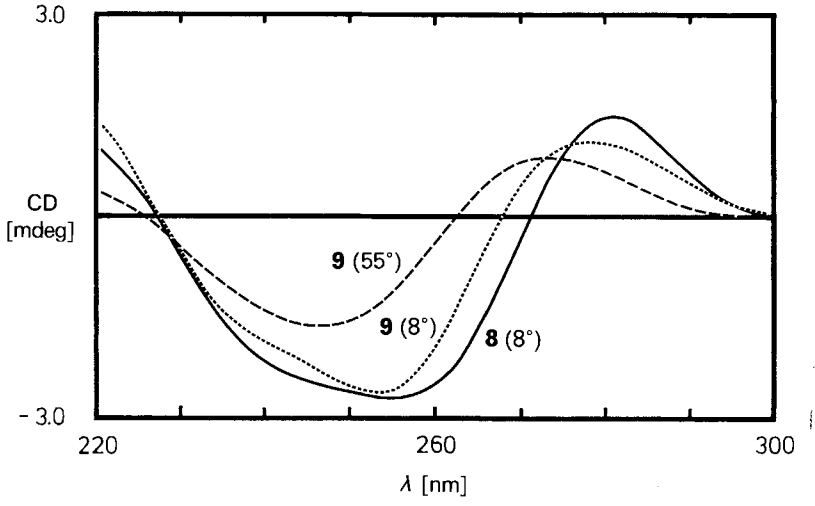

Fig. 5. *CD Spectra of d(G-T-A-G-A-A-xT-xT-C-T-A-C)$_2$* (**9**; ·····) *and d(G-T-A-G-A-A-T-T-C-T-A-C)$_2$* (**8**; ——) *at 8° and of* **9** *at 55°*. Oligomer conc., 1.2 μM of double strand; buffer, see *Fig. 1*.

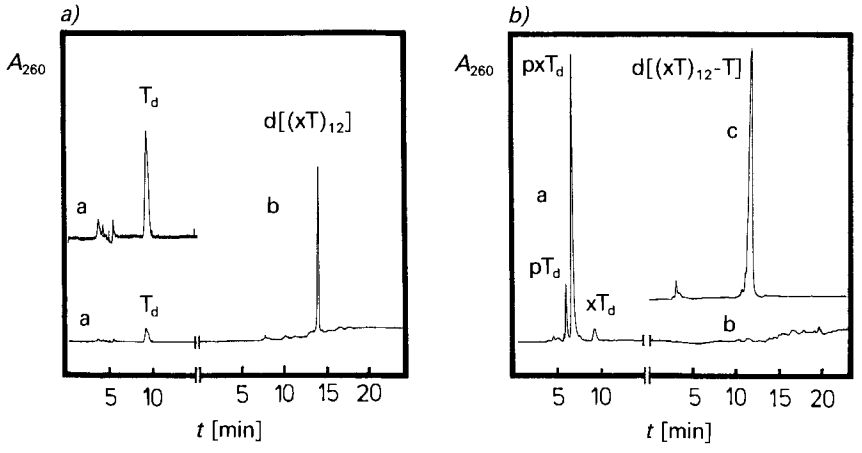

Fig. 6. *HPLC profiles of the products* a) *of calf-spleen phosphodiesterase hydrolysis of d[(xT)$_{12}$–T]* (**5**) *followed by alkaline-phosphatase treatment and* b) *of snake-venom phosphodiesterase hydrolysis of* **5**. Conditions, see *Exper. Part;* trace a, solvent system III; trace b, solvent system II, following solvent system III; trace c, d[(xT)$_{12}$ – T] (0.2 A_{260} units) with solvent system II.

calf-spleen phosphodiesterase (*Fig. 6a*); only the 3′-terminal 3′,4′-*erythro*-configurated T_d (t_R 9.3 min, solvent system III) was split off by the latter enzyme. A hydrolysis experiment on **5** with calf-spleen phosphodiesterase alone and subsequent HPLC analysis showed that again T_d and not its 5′-monophosphate pT_d was split off. The most likely interpretation of this result is that the enzyme skips the first twelve uncommon internucleotide linkages and acts formally as a 3′-exonuclease which offers the possibility to isolate d[(xT)$_{12}$]. As T_d and xT_d could not be separated by *RP-18* HPLC under standard elution conditions used for nucleoside analysis, we run the enzymatic cleavage experi-

ment of **5** also only with snake-venom phosphodiesterase with omission of alkaline phosphatase. As *Fig. 6b* shows, the liberated 5′-monophosphates of T_d and xT_d, *i.e.* pT_d and pxT_d, were now separated besides the formerly 5′-terminal xT_d confirming the cleavage of the oligo(2′-deoxyxylonucleotide).

We then studied the hydrolysis of the self-complementary oligomers **8** and **9** by both phosphodiesterases. Moreover, we followed the enzymatic cleavage spectrophotometrically at 296 K by taking advantage of the significant hypochromicities (*Table 2*) of both oligonucleotides. As *Fig. 7* shows, snake-venom phosphodiesterase hydrolyzed the modi-

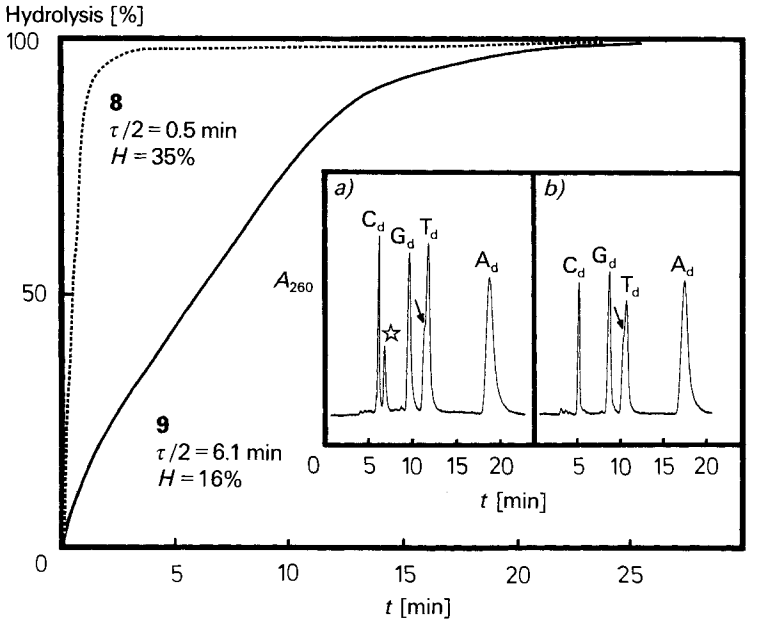

Fig. 7. *Time course of phosphodiester hydrolysis of d(G-T-A-G-A-A-xT-xT-C-T-A-C)$_2$* (**9**; ——), *and d(G-T-A-G-A-A-T-T-C-T-A-C)$_2$* (**8**; -----) *with snake-venom phosphodiesterase and alkaline phosphatase* (23°; conditions, see *Exper. Part;* 1.2 μM of each double strand) *and HPLC profiles* (insert) *after enzymatic tandem hydrolysis of* **9** *with snake-venom phosphodiesterase followed by alkaline phosphatase,* a) *after a total incubation of 75 min* (37°) *and* b) *after additional incubation for 30 min at 37°* (conditions, see *Exper. Part*). ☆: xT_d 5′-monophosphate (pxT_d); →: xT_d.

fied duplex **9** completely as well as the unmodified **8**, but with a twelvefold lower reaction rate. Interestingly, HPLC analysis (*Fig. 7a* (insert)) of the incubation mixture of **9** with snake-venom phosphodiesterase (45 min, 37°) followed by alkaline phosphatase (30 min, 37°) displays still a peak (t_R 6.3 min, solvent system III) of xT_d 5′-monophosphate (pxT_d; see *Fig. 6b*), indicating that alkaline phosphatase hydrolyzed this modified nucleotide with a significantly slower rate compared to the regular nucleoside 5′-monophosphates. Additional incubation for 30 min (37°) resulted in a complete hydrolysis of the modified nucleotide (*Fig. 7b* (insert)).

Figs. 8 and *9* show the time-dependent hydrolyses of **8** and **9** by calf-spleen phosphodiesterase and alkaline phosphatase: while the unmodified dodecamer **8** was hydrolyzed

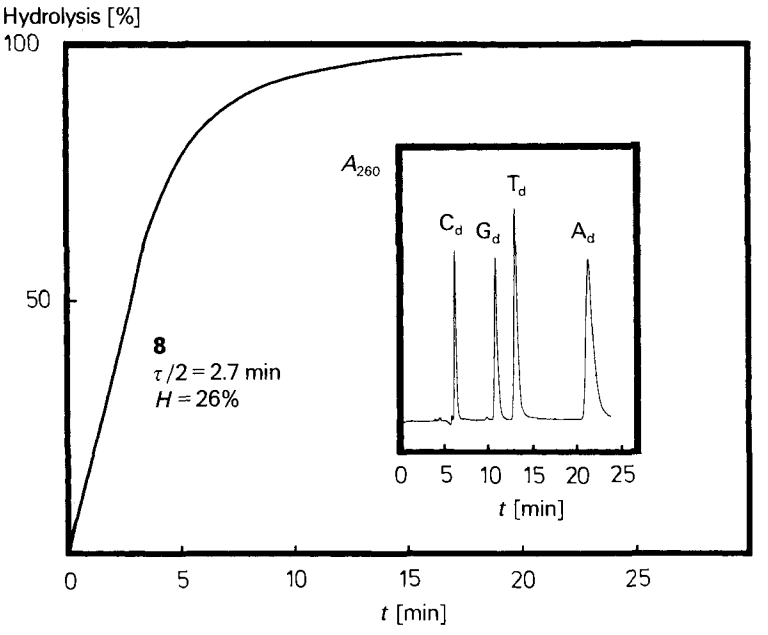

Fig. 8. *Time course of phosphodiester hydrolysis of d(G-T-A-G-A-A-T-T-C-T-A-C)$_2$* (**8**) *with calf-spleen phosphodiesterase and alkaline phosphatase* (23°; conditions, see *Exper. Part;* 1.2 μM of double strand) *and HPLC profile* (insert) *after enzymatic tandem hydrolysis of* **8** *with calf-spleen phosphodiesterase followed by alkaline phosphatase* (conditions, see *Exper. Part*).

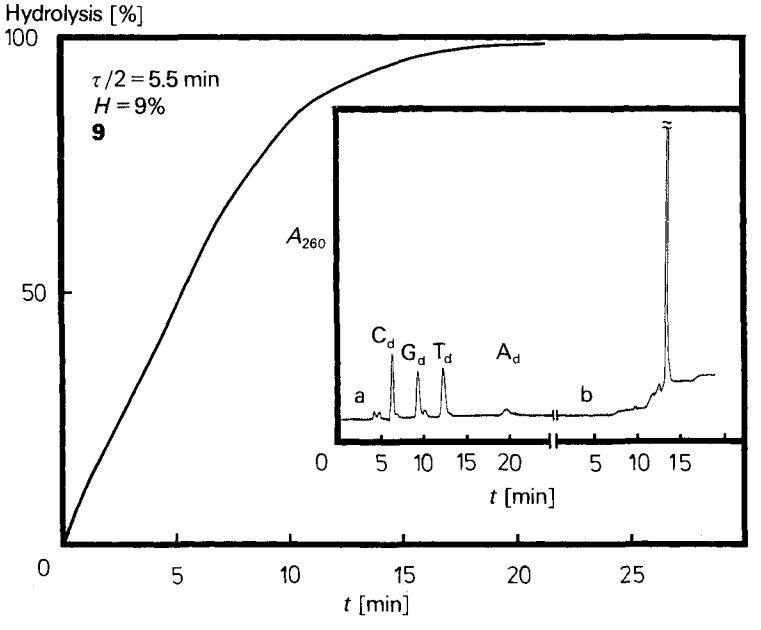

Fig. 9. *Time course of phosphodiester hydrolysis of d(G-T-A-G-A-A-xT-xT-C-T-A-C)$_2$* (**9**) *with calf-spleen phosphodiesterase followed by alkaline phosphatase* (23°; conditions, see *Exper. Part;* 1.2 μM of double strand) *and HPLC profile* (insert) *after enzymatic tandem hydrolysis of* **9** *with calf-spleen phosphodiesterase followed by alkaline phosphatase* (total incubation time, 2 h; 37°; conditions; see *Exper. Part*). Trace a, solvent system III; trace b, solvent system II, following solvent system III.

completely with a $\tau/2$ value of 2.7 min (296 K, *Fig. 8*), the modified oligonucleotide **9** was only partially hydrolyzed (*Fig. 9*). Obviously, calf-spleen phosphodiesterase was only able to cleave off a few 5′-terminal nucleotides with a $\tau/2$ value 5.5 min (hypochromicity, 9%). HPLC analysis reveals that most of the material was still in an oligomeric form (*Fig. 9* (insert): t_R 13 min, solvent system II). Unfortunately, we were not able to determine the exact composition of this residual oligonucleotide but could only show by HPLC, after further tandem hydrolysis with snake-venom phosphodiesterase and alkaline phosphatase, that it consisted of all regular nucleosides and xT_d. This residual oligomer was very resistant towards calf-spleen phosphodiesterase; as *Fig. 10* shows, it was still present in the enzymatic cleavage mixture after further incubation at 37° for 70 h. Within this time, the liberated A_d was already deaminated to 2′-deoxyinosine (I_d) by minute impurities of adenosine deaminase present in the purchased alkaline-phosphatase preparation (t_R of dI_d, 8.4 min, solvent system III).

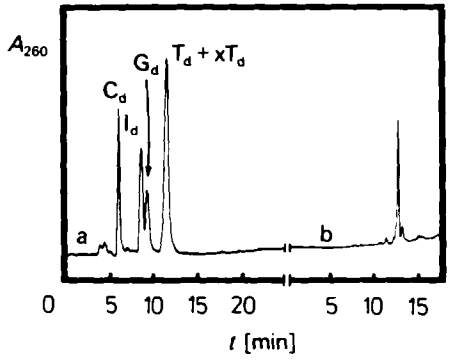

Fig. 10. *HPLC profile after enzymatic tandem hydrolysis of d(G-T-A-G-A-A-xT-xT-C-T-A-C)$_2$* (**9**; 1.2 μM of double strand) *with calf-spleen phosphodiesterase and alkaline phosphatase after a total incubation time of 70 h at 37°.* Trace a, solvent system III; trace b, solvent system II, following solvent system III. Conditions, see *Exper. Part.*

The first results on the synthesis and solution properties of oligo(2′-deoxyxylonucleotides) described in this manuscript opens a wide variety of experiments with these uncommon oligonucleotides with respect to their secondary structure, their hybridization with complementary DNA and RNA (anti-sense oligonucleotides) as well as their interaction with DNA-binding proteins. Such experiments and especially those on the protection of anti-sense oligonucleotides against their catabolic deactivation by cellular nucleases are under current investigation.

Experimental Part

General. See [17]. The phosphonates of regular 2′-deoxynucleosides were purchased from *Sigma*, St. Louis, and the *Fractosil*-linked 2′-deoxynucleosides from *Milligene*, Eschborn, Germany. Snake-venom phosphodiesterase (EC 3.1.15.1., *Crotallus durissus*), calf-spleen phosphodiesterase (EC 3.1.16.1.), and alkaline phosphatase (EC 3.1.3.1., *E. coli*) are products of *Boehringer*, Mannheim, Germany. Oligonucleotide synthesis was carried out on an automated DNA synthesizer, model *380 B*, of *Applied Biosystems*, Weiterstadt, Germany. CD Spectra: *Jasco 600* spectropolarimeter, thermostatically controlled 1-cm cuvettes connected with a *Lauda RCS 6* bath.

*1-(2′-Deoxy-β-*D-threo-*pentofuranosyl)thymine* (xT_d; **2**) was synthesized according to [4]. ^{1}H-NMR ((D$_6$)DMSO): 11.25 (br. *s*, NH); 7.80 (*s*, H–C(6)); 6.06 (*dd*, *J*(H–C(1′), H$_\beta$–C(2′)) = 2.7, *J*(H–C(1′), H$_\alpha$–C(2′)) = 6.5, H–C(1′)); 5.25 (OH–C(3′)); 4.69 (OH–C(5′)); 4.23 (*m*, H–C(3′)); 3.76 (*m*, H–C(4′)); 3.70 (*m*, CH$_2$(5′)); *ca.* 2.5 (H$_\alpha$–C(2′)); 1.84 (*d*, *J*(H$_\beta$–C(2′), H$_\alpha$–C(2′)) = −16.0, H$_\beta$–C(2′)).

*1-[2′-Deoxy-5′-*O*-(4,4′-dimethoxytriphenylmethyl)-β-*D-threo-*pentofuranosyl]thymine* (**3a**). By coevaporation with anh. pyridine (5 ml), **2** (500 mg, 2.06 mmol) was dried. The residue was dissolved in pyridine (15 ml) and stirred with 4,4′-dimethoxytriphenylmethyl chloride (1.02 g, 3 mmol) in the presence of (i-Pr)$_2$EtN (500 µl, 3 mmol) for 3 h at 40° under N$_2$. The soln. was then poured into 5% aq. NaHCO$_3$ soln. (50 ml), extracted with CH$_2$Cl$_2$ (2 × 100 ml), the combined org. extract dried (Na$_2$SO$_4$), and the solvent evaporated. After repeated coevaporation with toluene, the residue was purified by flash chromatography (FC; silica gel *60 H* (column 6 × 15 cm, CH$_2$Cl$_2$/MeOH 98:2): **3a** (780 mg, 69%). Colorless foam. TLC (silica gel, CH$_2$Cl$_2$/MeOH 95:5): R_f 0.6. ^{1}H-NMR ((D)$_6$DMSO): 11.30 (*s*, NH); 7.62 (*s*, H–C(6)); 7.45–6.86 (*m*, 13 arom. H); 6.12 (*dd*, *J* = 6.2, 2.7, H–C(1′)); 5.22 (*d*, *J* = 3.4, OH–C(3′)); 4.20 (*m*, H–C(3′)); 4.10 (*m*, H–C(4′)); 3.73 (*s*, 2 MeO); 3.40, 3.19 (2*m*, CH$_2$(5′)); *ca.* 2.51 (*m*, H$_\alpha$–C(2′)); 1.87 (*d*, *J* = −15.4, H$_\beta$–C(2′)); 1.66 (*s*, Me). Anal. calc. for $C_{31}H_{32}N_2O_7$ (544.6): C 68.37, H 5.92, N 5.14; found: C 68.44, H 6.00, N 5.15.

*1-[(2′-Deoxy-5′-*O*-(4,4′-dimethoxytriphenylmethyl)-β-*D-threo-*pentofuranosyl)]thymine 3′-(Triethylammonium Phosphonate)* (**3b**). To a soln. of PCl$_3$ (400 µl, 4.6 mmol) and *N*-methylmorpholine (5.1 ml, 46 mmol) in CH$_2$Cl$_2$ (36 ml) was added 1,2,4-triazole (1.06 g, 15.3 mmol). After stirring for 30 min, the soln. was cooled to 0°, and **3a** (500 mg, 0.92 mmol) which had been dried by evaporation from anh. MeCN and dissolved in CH$_2$Cl$_2$ (12 ml) was added slowly. After stirring for 10 min at r.t., the mixture was poured into 1M aq. (Et$_3$NH)HCO$_3$ (*TBK*; pH 8.0; 50 ml), shaken, and separated. The aq. layer was extracted with CH$_2$Cl$_2$ (30 ml), the combined org. extract dried (Na$_2$SO$_4$) and evaporated, and the colorless foam submitted to FC (silica gel *60 H*, column 6 × 15 cm, CH$_2$Cl$_2$/Et$_3$N 92:8 (1 l), then CH$_2$Cl$_2$/MeOH/Et$_3$N 88:10:2). The residue of the main zone was dissolved in CH$_2$Cl$_2$ (15 ml) and extracted twice with 1M aq. (Et$_3$NH)HCO$_3$ (20 ml; pH 8.0). The org. layer was dried (Na$_2$SO$_4$) and evaporated: **3b** (480 mg, 74%). Colorless foam. TLC (silica gel, CH$_2$Cl$_2$/MeOH/Et$_3$N, 88:10:2): R_f 0.3. ^{1}H-NMR ((D$_6$)DMSO): 11.30 (*s*, NH); 7.66 (*s*, H–C(6)); 7.63–6.86 (*m*, 13 arom. H); 6.13 (*dd*, *J* = 6.8, 2.8, H–C(1′)); 5.76, 5.28 (*d*, *J* = 119, PH); 4.62 (*m*, H–C(3′)); 4.12 (*m*, H–C(4′)); 3.73 (*s*, 2 MeO); 3.34, 3.16 (*m*, CH$_2$(5′)); 2.73 (*q*, CH$_3$C*H*$_2$NH); *ca.* 2.5 (*m*, H$_\alpha$–C(2′)); 2.14 (*d*, *J* = −15.2, H$_\beta$–C(2′)); 1.66 (*s*, Me); 1.03 (*t*, C*H*$_3$CH$_2$NH). ^{31}P-NMR ((D$_6$)DMSO): 0.88 (^1J(P,H) = 587, ^3J(P,H–C(4′)) = 8.8). Anal. calc. for $C_{37}H_{48}N_3O_9P$ (709.8): C 62.61, H 6.82, N 5.92; found: C 62.81, H 7.00, N 5.99.

*1-[2′-Deoxy-5′-*O*-(4,4′-dimethoxytriphenylmethyl)-β-*D-threo-*pentofuranosyl]thymine 3′-[(2-Cyanoethyl)* N,N-*Diisopropylphosphoramidite]* (**3c**). To a soln. of **3a** (100 mg, 0.18 mmol) and (i-Pr)$_2$EtN (100 µl, 0.57 mmol) in dry THF, chloro(2-cyanoethoxy)(diisopropylamino)phosphane (45 µl, 0.2 mmol) was added within 2 min at r.t. under N$_2$. After stirring for 30 min, the reaction was quenched by adding 5% aq. NaHCO$_3$ soln. (4 ml). The mixture was extracted with CH$_2$Cl$_2$ (2 × 5 ml) and the org. layer dried (Na$_2$SO$_4$) and evaporated. FC (silica gel *60 H*, column 3 × 6 cm, AcOEt/CH$_2$Cl$_2$/Et$_3$N 45:45:10) gave two partially overlapping zones of diastereoisomers **3c** (95 mg, 72%). TLC (silica gel, CH$_2$Cl$_2$/AcOEt/Et$_3$N 45:45:10): R_f 0.7 and 0.6. ^{31}P-NMR (CDCl$_3$): 148.5 (faster migrating zone); 151.8 (slower migrating zone).

*1-[2′-Deoxy-5′-*O*-(4,4′-dimethoxytriphenylmethyl)-3′-*O*-β-*D-threo-*pentofuranosyl]thymine 3′-(3-Carboxypropanoate)* (**4a**). To a soln. of **3a** (250 mg, 0.46 mmol) in dry pyridine (10 ml), 4-(dimethylamino)pyridine (70 mg, 0.54 mmol) and succinic anhydride (230 mg, 2.3 mmol) were added. The mixture was stirred for 70 h at 40°. H$_2$O (3 ml) was added, the mixture evaporated and coevaporated with toluene to remove pyridine, the resulting oil dissolved in CH$_2$Cl$_2$ and washed with 10% aq. citric acid and H$_2$O, and the org. layer dried (Na$_2$SO$_4$) and evaporated. The residue was dissolved in CH$_2$Cl$_2$/pyridine 95:5 (2 ml) and added slowly to pentane/Et$_2$O 1:1 (50 ml). The precipitate was filtered off and submitted to FC (silica gel *60*, column 10 × 6 cm, 0.7 bar). MeCN/H$_2$O (9:1) eluted one main zone: **4a** (180 mg, 61%). Colorless powder. TLC (silica gel, MeCN/H$_2$O 9:1): R_f 0.8. ^{13}C-NMR ((D$_6$)DMSO): 173.6, 171.2 (2 C=O); 163.8 (C(6)); 158.3 ((MeO)$_2$*Tr*); 150.5 (C(2)); 144.7 ((MeO)$_2$*Tr*);

135.5 (C(4)); 135.4–126.9 (10 signals, $(MeO)_2Tr$); 113.3 (quart. C, $(MeO)_2Tr$); 109.0 (C(5)); 85.8 ($(MeO)_2Tr$); 83.6 (C(4')); 80.6 (C(1')); 72.3 (C(3')); 61.2 (C(5')); 55.1 ($(MeO)_2$Tr); 40.6 (C(2')); 29.1, 29.0 (2 CH_2); 12.3 (*Me* of Thy).

*1-(2'-Deoxy-β-*D*-*threo*-pentofuranosyl)thymine 3'-[3-(*N*-'Fractosil'carbamoyl)propanoate]* (**4c**). To a soln. of **4a** (100 mg, 0.16 mmol) in 1,4-dioxane/pyridine 95:5 (1 ml), 4-nitrophenol (40 mg, 0.29 mmol), and *N,N*-dicyclohexylcarbodiimide (60 mg, 0.3 mmol) were added under stirring at r.t. After 2 h, dicyclohexylurea was removed by filtration. To the filtrate, *Fractosil 200* (200 mg, 450 μequiv. NH_2/g) and DMF (1 ml) were added. After addition of Et_3N (200 μl), the suspension was shaken for 4 h at r.t. Then Ac_2O (60 μl) was added and shaking was continued for another 30 min. The *Fractosil* derivative **4c** was filtered off, washed with DMF, EtOH, and Et_2O, and dried *in vacuo*. The amount of silica gel bound nucleoside was determined by treatment of **4c** (5 mg) with 0.1M TsOH (10 ml) in MeCN. From the absorbance at 498 nm of the supernatant, 50.4 μmol of linked **2**/g *Fractosil* was calculated ($\varepsilon((MeO)_2Tr) = 70000$).

Solid-Phase Synthesis of the Oligomers **5–9**. The synthesis of the oligonucleotides was accomplished on a 1-μmol scale using the 3'-phosphonates of $[(MeO)_2Tr]bz^6A_d$, $[(MeO)_2Tr]ib^2G_d$, $[(MeO)_2Tr]bz^4C_d$, and $[(MeO)_2Tr]T_d$ as well as compound **3b**. The synthesis of **5–9** followed the regular protocol of the DNA synthesizer for 3'-phosponates [18]. Deprotection of NH_2 groups was carried out with 25% aq. NH_3 soln. at 60° for 48 h. The 4,4'-dimethoxytrityl residues of the oligomers were removed by treatment with 80% AcOH for 5 min at r.t. Purification was accomplished by HPLC (see below) on *RP-18* columns using solvent system I for the $(MeO)_2Tr$ derivatives of the oligonucleotides, and II for the detritylated oligomers. The oligonucleotides were desalted on a 4 × 25 mm HPLC cartridge (*RP-18* silica gel). Inorg. material was eluted with H_2O (10 ml), while the oligomer was eluted with MeOH/H_2O 3:2 (5 ml). The oligomers were lyophilized on a *Speed-Vac* evaporator to yield a colorless foam which was dissolved in H_2O (100 μl) and stored frozen at −18°.

Enzymatic Hydrolysis of the Oligomers and Hypochromicity. The oligonucleotides (0.2 A_{260} units) were dissolved in 0.1M *Tris*-HCl buffer (pH 8.3; 200 μl) and treated with either snake-venom phosphodiesterase (6 μg) at 37° for 45 min and alkaline phosphatase (2 μg) for 30 min at 37° or with calf-spleen phosphodiesterase (12 μg) and alkaline phosphatase. The mixture was analyzed on reversed-phase HPLC (*RP-18*, solvent system III, followed by solvent system II; see below). Quantification of the material was made on the basis of the peak areas which were divided by the extinction coefficients of the nucleoside constituents (ε_{260}: A_d, 15400; C_d, 7300; G_d, 11700; T_d, xT_d, 8800).

Hypochromicity values of **6–8** (*Table 2*) were determined by enzymatic degradation of *ca.* 0.5 A_{260} units of the corresponding oligonucleotide as described above. The hyperchromicity of the oligomer is defined as the value of the final absorbance at 260 nm divided by the initial absorbance. The extinction coefficient of the oligonucleotide is the sum of the extinction coefficients of the constituent monomeric deoxynucleosides divided by hyperchromicity. Then, the hypochromicity values were calculated using the equation: $H = [(\varepsilon_{monomer} - \varepsilon_{oligomer}) \cdot (\varepsilon_{monomer})^{-1}] \cdot 100\%$ [19].

Time courses of phosphodiester hydrolysis of oligonucleotides were measured as follows: The appropriate oligonucleotide (1.2 μM of double strand) was dissolved in 0.1M *Tris*-HCl buffer (pH 8.3), and alkaline phosphatase (2 μg) was added. Reaction was started by addition of either snake-venom phosphodiesterase (6 μg) or calf-spleen phosphodiesterase (12 μg). The increase of A_{260} was continuously measured in thermostatted quartz cuvettes (1-cm path length) at 23°; the end absorbance was normalized to 100% of hydrolysis.

HPLC Separation. HPLC was carried out on a 4 × 250 and 4 × 25 mm (10 μm) *RP-18 Lichrosorb* column (*Merck*) using a *Merck-Hitachi* HPLC apparatus with one pump (model *655 A-12*) connected with a proportioning valve, a variable-wavelength monitor (model *655 A*), and a controller (model *L-5000*), connected with an integrator (model *D-2000*). The solvent systems consisting of 0.1M (Et_3NH)OAc (pH 7)/MeCN 95:5 (*A*) and MeCN (*B*) were used in the following order: solvent system I, 3 min 15% *B* in *A*, 7 min 15–40% *B* in *A*, 5 min 40% *B* in *A*, 5 min 40–15% *B* in *A*, flow rate 1 ml/min; solvent system II, 20 min 0–20% *B* in *A*, flow rate 1 ml/min; solvent system III 15 min 100% *A*, flow rate 0.6 ml/min.

Melting Experiments. The melting experiments were carried out in a thermostatically controlled cell holder with a *Shimadzu-210-A* UV spectrophotometer connected with a *Kipp and Zonen BD 90* recorder. The increase of absorbance at either 260 or 284 nm as a function of time was recorded, while the temp. of the soln. was increased linearily (10–80°) with time at a rate of 20°/h using a *Lauda PM-350* programmer and a *Lauda RCS 6* bath equipped with a *R22* unit (*MWG Lauda*, Germany). The actual temp. was measured in the reference cell with a Pt resistor. Melting hypochromicity values were calculated from the initial and final absorbances as described above.

The authors gratefully acknowledge excellent technical assistance by Miss *Iris Strodtholz* as well as financial support by the *Deutsche Forschungsgemeinschaft*.

REFERENCES

[1] F. Morvan, B. Rayner, J.-L. Imbach, S. Thenet, J. R. Bertrand, J. Paoletti, C. Malvy, C. Paoletti, *Nucleic Acids Res.* **1988,** *15,* 3421.

[2] A. Eschenmoser, 'Ber. der Gesellschaft Deutscher Naturforscher und Ärzte, Berlin, Sept. 1990.

[3] N. I. Sokolova, N. G. Dolinnaya, N. F. Krynetskaya, Z. A. Shabarova, *Nucleos. Nucleot.* **1990,** *9,* 515.

[4] J. J. Fox, N. C. Miller, *J. Org. Chem.* **1963,** *28,* 936.

[5] B. C. Froehler, P. G. Ng, M. D. Matteucci, *Nucleic Acids Res.* **1986,** *14,* 5399.

[6] C. Altona, M. Sundaralingam, *J. Am. Chem. Soc.* **1972,** *94,* 8205.

[7] C. A. G. Haasnoot, F. A. A. M. de Leeuw, H. P. M. de Leeuw, C. Altona, *Org. Magn. Reson.* **1981,** *15,* 43.

[8] L. M. Koole, H. M. Buck, A. Nyilas, J. Chattopadhyaya, *Can. J. Chem.* **1987,** *65,* 2089.

[9] H. Rosemeyer, F. Seela, *Helv. Chim. Acta* **1989,** *72,* 1084.

[10] F. Seela, H. Driller, *Helv. Chim. Acta* **1988,** *71,* 1191.

[11] F. Seela, H. Driller, *Nucleic Acids Res.* **1986,** *14,* 2319.

[12] N. Camerman, J. K. Fawcett, A. Camerman, *J. Mol. Biol.* **1976,** *107,* 601.

[13] W. Saenger, in 'Principles of Nucleic Acid Structure', Ed. C. R. Cantor, Springer Verlag, New York, 1984, p. 294.

[14] D. S. Pilch, C. Levenson, R. H. Shafer, *Proc. Natl. Acad. Sci. U.S.A.* **1990,** *87,* 1942.

[15] W. Saenger, in 'Principles in Nucleic Acid Structure', Ed. C. R. Cantor, Springer Verlag, New York, 1984, p. 284.

[16] W. Saenger, in 'Principles in Nucleic Acid Structure', Ed. C. R. Cantor, Springer Verlag, New York, 1984, p. 371.

[17] F. Seela, K. Kaiser, U. Bindig, *Helv. Chim. Acta* **1989,** *72,* 868.

[18] *Applied Biosystems,* 'Users Manual of the DNA Synthesizer' *380B.*

[19] P. C. Newman, V. U. Nwosu, D. M. Williams, R. Cosstick, F. Seela, B. A. Connolly, *Biochemistry* **1990,** *29,* 9891.